ELSEVIER

Thermochimica Acta 293 (1997) 13–24

thermochimica acta

High-temperature Raman spectroscopic studies on nickel iodates[1]

G. Pracht, N. Lange, H.D. Lutz*

Anorganische Chemie I, Universität Siegen, D-57068 Siegen, Germany

Received 4 November 1996

Abstract

The phase relationships of the nickel iodate–water system have been examined using thermal analyses (DSC), X-ray, IR and Raman spectroscopic methods, and especially high-temperature Raman and high-temperature X-ray experiments. The compounds established are $Ni(IO_3)_2 \cdot 10H_2O$, which has been obtained for the first time (ν_{OD} of matrix isolated HDO molecules in isotopically diluted samples: 2585, 2549, 2521, 2480, 2451, 2442, 2431, 2374, 2354, 2341 and 2295 cm^{-1}, 95 K), α-$Ni(IO_3)_2 \cdot 4H_2O$, β-$Ni(IO_3)_2 \cdot 4H_2O$ (2443 and 2378 cm^{-1}, 95 K), $Ni(IO_3)_2 \cdot 2H_2O$ (2515 and 2427 cm^{-1}, 95 K), α-$Ni(IO_3)_2$, and β-$Ni(IO_3)_2$. The IO stretching modes of nickel iodates resemble those of other solid iodates, whereas the bending modes are reinforced by up to 100 cm^{-1}, e.g. for α-$Ni(IO_3)_2$ with $\nu_2 = 452$ and 463 cm^{-1}. $Ni(IO_3)_2 \cdot 10H_2O$ (space group $P\bar{1}$, unit cell dimensions: $a = 650.02(12)$, $b = 1098.54(22)$, $c = 1169.21(19)$ pm, $\alpha = 105.654(11)^\circ$, $\beta = 103.856(11)^\circ$ and $\gamma = 101.515(11)^\circ$) is isostructural to the respective magnesium compound. Decomposition and phase transition occur as follows: $Ni(IO_3)_2 \cdot 10H_2O$ (314 K, DSC)$\rightarrow$$\beta$-$Ni(IO_3)_2 \cdot 4H_2O$ (421 K)$\rightarrow$$Ni(IO_3)_2 \cdot 2H_2O$ (431 K)$\rightarrow$$\alpha$-$Ni(IO_3)_2$ (745 K)$\rightarrow$$\beta$-$Ni(IO_3)_2$ (790 K)$\rightarrow$$NiO+I_2+O_2$, or α-$Ni(IO_3)_2 \cdot 4H_2O$ (384 K)$\rightarrow$$Ni(IO_3)_2 \cdot 2H_2O\rightarrow$, etc. Decomposition to the oxide instead of the iodide is favoured by the high stability of transition metal oxides. © 1997 Elsevier Science B.V.

Keywords: High-temperature Raman spectra; Nickel iodate hydrates; Phase relationships; Raman and infrared spectra; Thermal analyses; X-ray powder data

1. Introduction

On heating hydrated and unhydrated iodates, disproportionation to periodates and iodides or decomposition to the respective oxides under evolution of oxygen and iodine occur depending on which metal ions are involved [1–3]. In order to establish the relevant properties of the various metals, we perform systematic studies on metal iodates. In addition to conventional thermal analyses (DTA, DSC, TG), high-temperature Raman spectroscopy and high-temperature X-ray diffraction studies are valuable tools for illuminating the phase relationships of such systems.

In the nickel iodate–water system, $Ni(IO_3)_2 \cdot 7.45H_2O$ [4], two polymorphic tetrahydrates [5–10], two dihydrates [5–8,10–15], and two polymorphic anhydrous salts [5–8,10,16,17] have been reported in the literature. These compounds, however, are only poorly characterised with respect to spectroscopic data, stability of the various polymorphs, decomposition, dehydration, and phase transition. We therefore studied the system under discussion by means of

*Corresponding author. Tel.: 0271/740-4217/4218; fax: 0271/7402555.

[1]This work is dedicated to professor Welf Bronger on the occasion of his 65th birthday

PII S0040-6031(97)00013-0

thermoanalytic, X-ray, IR and Raman spectroscopic methods.

2. Experimental

2.1. Preparation

The starting materials were the various hydrates of nickel iodate including hitherto unknown $Ni(IO_3)_2 \cdot 10H_2O$. They (as well as deuterated specimens) were prepared by crystallisation of aqueous solutions as given below.

2.1.1. $Ni(IO_3)_2 \cdot 10H_2O$

Needle-shaped crystals of $Ni(IO_3)_2 \cdot 10H_2O$ were obtained from an aqueous solution of HIO_3 or KIO_3 (1 M) and a freshly prepared solution of $Ni(NO_3)_2$ (2 M). In order to prevent precipitation of amorphous products, the solutions were freezed in with liquid nitrogen in a 100 ml flask in the following sequence: 60 ml HIO_3, 10 ml H_2O, 20 ml $Ni(NO_3)_2$, 10 ml H_2O, and 10 ml ethanol. The solution should contain an excess of iodic acid. The frozen solution was then thawed in a refrigerator at 268 K within 10 h. The precipitate was strained off and washed with ethanol and acetone. $Ni(IO_3)_2 \cdot 10H_2O$ can be stored at 268 K for a short time.

2.1.2. α-$Ni(IO_3)_2 \cdot 4H_2O$, β-$Ni(IO_3)_2 \cdot 4H_2O$, $Ni(IO_3)_2 \cdot 2H_2O$, α- and β-$Ni(IO_3)_2$

Following Nassau et al. [7], α-$Ni(IO_3)_2 \cdot 4H_2O$ was prepared from solutions of iodic acid and nickel nitrate in a refrigerator at 275 K. In order to obtain α-$Ni(IO_3)_2 \cdot 4H_2O$ instead of $Ni(IO_3)_2 \cdot 10H_2O$, the $Ni(NO_3)_2$ solution used should not be the one freshly prepared, but one left standing for some days. If the solution with the α-$Ni(IO_3)_2 \cdot 4H_2O$ precipitate remains unstrained for some days, a small portion converts to β-$Ni(IO_3)_2 \cdot 4H_2O$. Crystals of β-$Ni(IO_3)_2 \cdot 4H_2O$ were prepared from iodic acid and nickel nitrate using gel-crystallisation techniques in U-shaped pipes at 293 K.

$Ni(IO_3)_2 \cdot 2H_2O$ and green coloured α-$Ni(IO_3)_2$ were prepared by dehydration of β-$Ni(IO_3)_2 \cdot 4H_2O$ at 413 K and of $Ni(IO_3)_2 \cdot 2H_2O$ at 473 K, respectively, as shown in the following. Yellow β-$Ni(IO_3)_2$ is obtained (i) by heating α-$Ni(IO_3)_2$ above 753 K, partly under decomposition to NiO and I_2, (ii) from an aqueous $Ni(IO_3)_2$ solution in an autoclave at ~470 K, and (iii) by crystallisation from an aqueous nitric acid solution of $Ni(NO_3)_2$ and HIO_3 at 373 K.

2.2. Apparatus and techniques

DSC (differential scanning calorimetry) measurements were performed with 5–12 mg of the sample in a dry nitrogen stream using a Perkin–Elmer DSC 7 calorimeter with aluminium pans as sample holders. The heating rates were 5 and 10 K min^{-1}. An empty pan was used as reference.

Raman spectra, with the sample in closed glass capillaries, were measured on a Dilor OMARS 89 multichannel Raman spectrograph (resolution $< 4\ cm^{-1}$) using the right-angle geometry. The 514.5 nm line of an argon-ion laser was employed for excitation. The wavenumbers of the observed bands were calibrated by means of the plasma lines of the laser used. Low-temperature Raman spectra were recorded with the use of the variable temperature cell Coderg model CRN2 (100–300 K). A special high-temperature cell was used with the Eurotherm PID controller 818b and the Eurotherm thyristor controlling unit 425 for the high-temperature spectra (HT-Raman), with the samples in open glass capillaries. More details are given elsewhere [18,19]. The samples were warmed in steps of 2 K, in the case of $Ni(IO_3)_2 \cdot 10H_2O$, and in steps of 5–10 K for all other compounds. For each spectrum, the cell was kept at constant temperature for 5-10 min.

IR- and FIR-spectra were recorded on a Bruker IFS 113v spectrometer (resolution $<2\ cm^{-1}$) using KBr discs, fluorolube and Nujol mulls. For the low-temperature spectra (liquid nitrogen), the variable temperature cell Graseby Specac P/N 21.500 (with an Eurotherm controller 808) was used.

High-temperature X-ray diffraction patterns (HT-X-ray) (80–873 K) were obtained with an Enraf-Nonius FR 553 Guinier Simon camera (Cu $K\alpha_1$ radiation, Si as internal standard, heating rates of 5 and 10 K h^{-1}). X-ray powder diffractograms were recorded on a Siemens D5000 diffractometer in transmission geometry with primary monochromator and a Braun PSD-50M detector. Unit-cell dimensions and diffraction patterns were computed by the LSUCR [20] and Lazy Pulverix [21] programmes, respectively.

3. Results

3.1. Spectroscopic and structural properties of nickel iodates

Raman and infrared spectra of the various nickel iodates are shown in Figs. 1–8. The various polymorphs are labelled as reported by Nassau et al. [7]. The infrared spectra of the lower hydrates and the anhydrous $Ni(IO_3)_2$ polymorphs reported in the literature [7] are almost confirmed. (The spectra of α- and β-$Ni(IO_3)_2{\cdot}4H_2O$ given in Fig. 12 and Fig. 13 of [7], however, have been interchanged.)

The vibrational spectra and the X-ray powder data of $Ni(IO_3)_2{\cdot}10H_2O$ reveal that the novel compound, which corresponds to $Ni(IO_3)_2{\cdot}7.45H_2O$ reported by Weigel et al. [4], is isostructural with the recently established $Mg(IO_3)_2{\cdot}10H_2O$ [22] (see Figs. 1 and 9). The X-ray powder data of this triclinic compound (space group $P\bar{1}$) were indices in analogy to isostructural $Mg(IO_3)_2{\cdot}10H_2O$: $a = 650.02(12)$, $b = 1098.54(22)$, $c = 1169.21(19)$pm, $\alpha = 105.654(11)°$, $\beta = 103.856(11)°$, and $\gamma = 101.515(11)°$. There are twenty crystallographically different hydrogen positions in the structure. The IR- and Raman spectra in the O–D stretching mode region show 11 different bands of matrix isolated HDO molecules (ν_{OD}: 2585, 2549, 2521, 2480, 2451, 2442, 2431, 2374, 2354, 2341, 2295 cm^{-1}, 95 K) (see Figs. 1 and 3).

The X-ray powder photographs of α-$Ni(IO_3)_2{\cdot}4H_2O$ [5–7,10], which are of poor quality, could not be indexed (see Table 1). It belongs to an hitherto

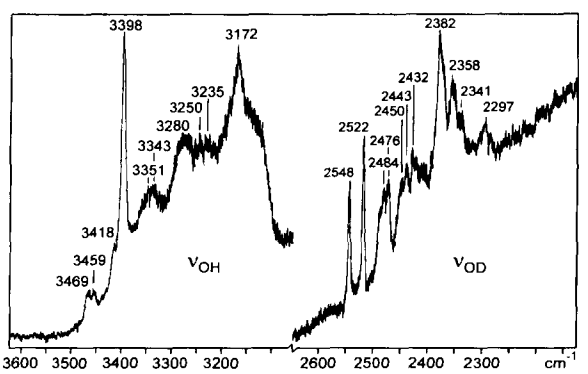

Fig. 1. Raman spectra of $Ni(IO_3)_2{\cdot}10H_2O$ (deuterated by 10%), in the ν_{OH} and ν_{OD} mode region at 90 K.

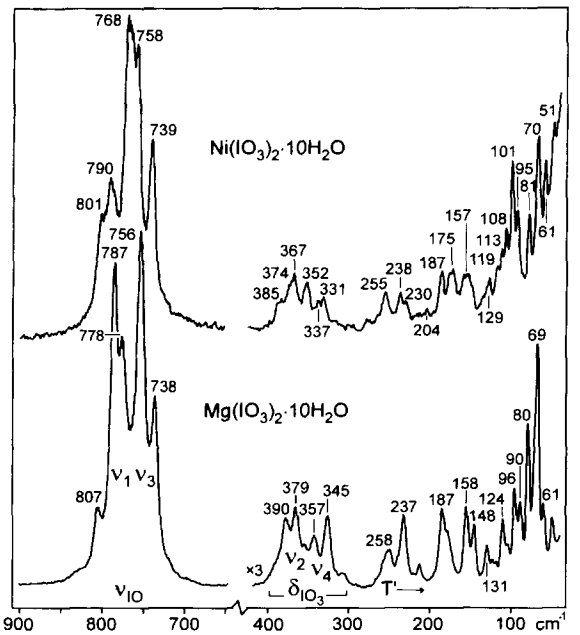

Fig. 2. Raman spectra of $Ni(IO_3)_2{\cdot}10H_2O$ and isostructural $Mg(IO_3)_2{\cdot}10H_2O$ [22] at 90 K in the 50–900 cm^{-1} range (ν_{IO}, ν_1, ν_3 – IO stretching modes; δ_{IO3}, ν_2, ν_4 – IO_3 bending modes; and T' – translational modes).

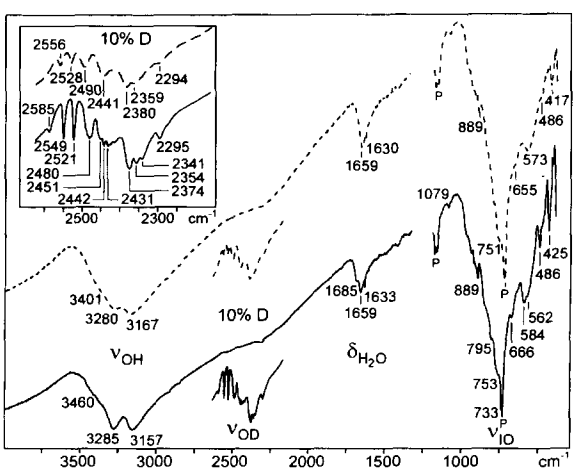

Fig. 3. Infrared spectra (fluorolube and paraffin mulls) of $Ni(IO_3)_2{\cdot}10H_2O$ (0 and 10% D) in the ν_{OH}, ν_{OD}, δ_{H2O} and ν_{IO} mode region of the H_2O (and matrix isolated HDO) molecules and the IO_3^- ions (dashed line – 260 K; full line – 90 K; and P – peaks due to paraffin mull).

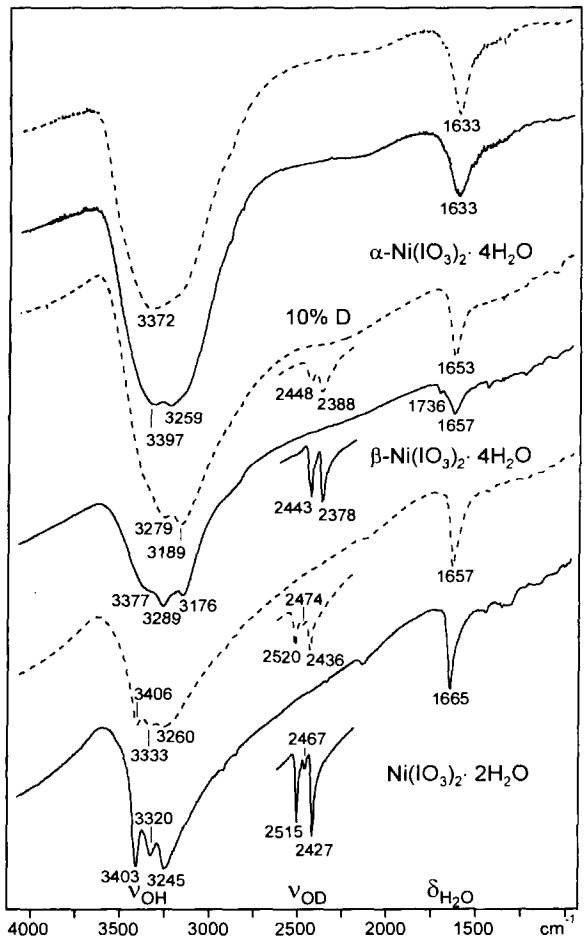

Fig. 4. Infrared spectra (KBr discs) of the lower hydrates of $Ni(IO_3)_2$ (0 and 10%D) at 90 and 300 K (dashed line) in the ν_{OH}, ν_{OD}, and δ_{H_2O} mode region (for further explanations see Fig. 3).

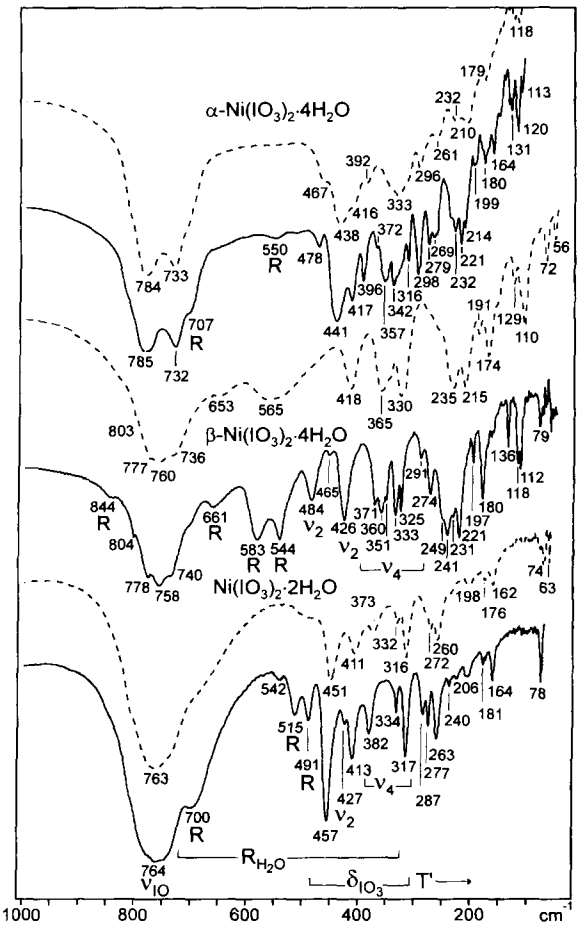

Fig. 5. Infrared spectra (KBr discs and paraffin mulls) of the lower hydrates of $Ni(IO_3)_2$ at 90 and 300 K in the 50–1000 cm^{-1} range (R_{H_2O} – liberation of the water molecules; for further explanations see Figs. 2–4).

unknown structure type. The water bands observed in this work (ν_{OH} ~3397 and 3259 cm^{-1}, see Fig. 4) somewhat differ from those (3140 cm^{-1}) reported by Nassau et al. [7]. Deuterated samples of this hydrate could not be obtained. β-$Ni(IO_3)_2{\cdot}4H_2O$ [6–10], which was reported by Meuser as α-$Ni(IO_3)_2{\cdot}2H_2O$, is isostructural to monoclinic $M(IO_3)_2{\cdot}4H_2O$ (M=Mg, Co) [22,23]. In contrast to isotypic $Mg(IO_3)_2{\cdot}4H_2O$, the four uncoupled OD stretching modes due to the four hydrogen positions of the structure [23] could not be fully resolved (see Fig. 4).

$Ni(IO_3)_2{\cdot}2H_2O$ [6–8,10–12], which is Meuser's β-$Ni(IO_3)_2{\cdot}2H_2O$, crystallises in the orthorhombic space group Pbca [13,14]. The two hydrogen positions of the crystallographically equal water molecules correspond to the OD stretching modes (matrix isolated HDO) at 2515 and 2427 cm^{-1} (95 K). The weak OD stretching mode at 2467 cm^{-1} cannot be assigned; possibly, it belongs to hitherto unknown hydrate. However, a second polymorph of the dihydrate [11] could not be established.

The relative large number of IR- and Raman bands of green coloured α-$Ni(IO_3)_2$ [7,10,16] (see Figs. 7 and 8) evidences a large unit cell with at least four formula units. The isotypism with α-$Cu(IO_3)_2$

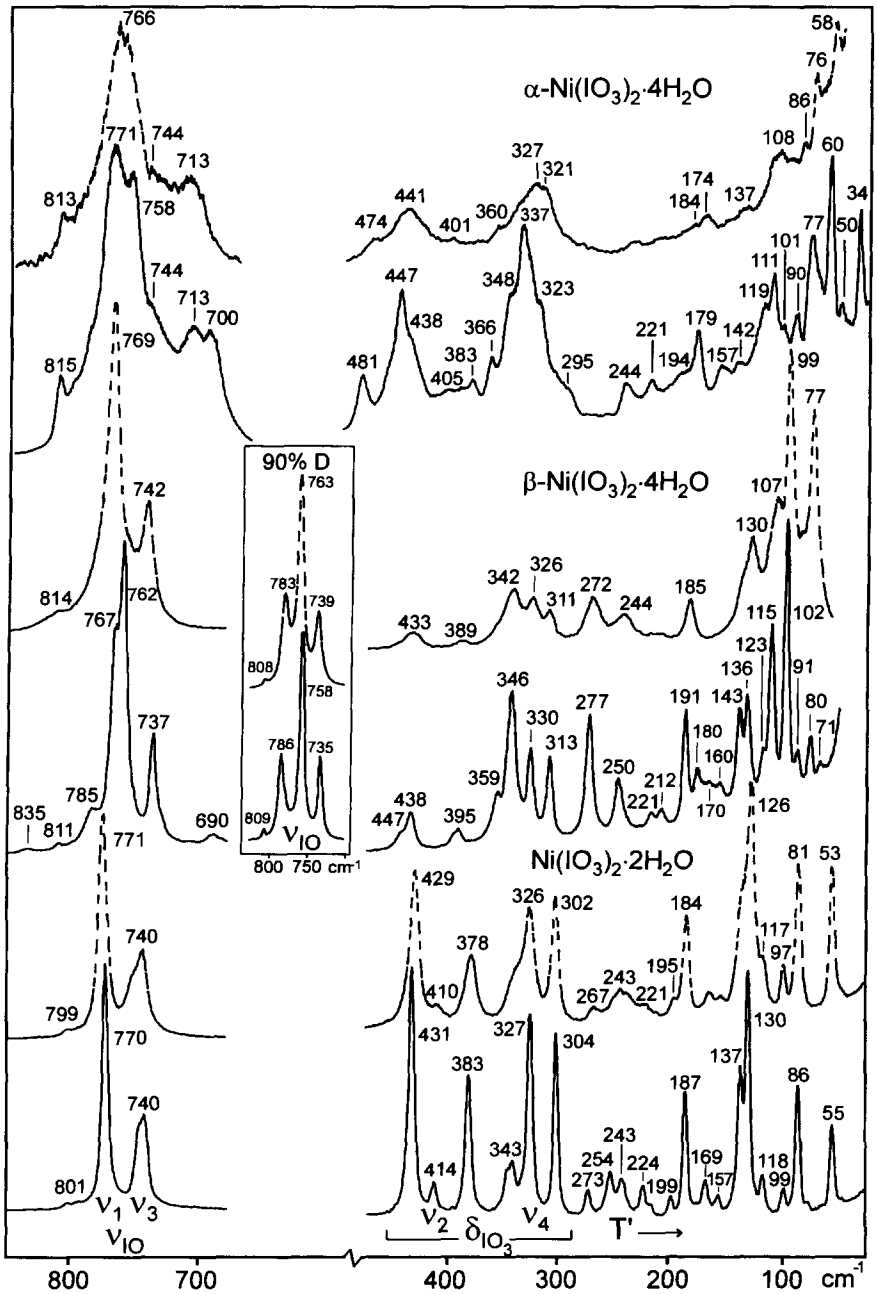

Fig. 6. Raman spectra of the lower hydrates of nickel iodates at 90 and 300 K in the 50–900 cm^{-1} range; the unmixed ν_{IO} bands (with R_{H_2O}) are only shown in the spectra of highly deuterated samples (for further explanations see Figs. 2–4).

reported in [16] must therefore be doubted (see Table 2). Yellow coloured β-$Ni(IO_3)_2$ [5–7,10,17] crystallises in the hexagonal space group $P6_3$ or $P6_322$ [10]. The proposed structure is compatible with the obtained IR and Raman spectra. β-$Ni(IO_3)_2$ is isostructural to $Mg(IO_3)_2$ (see Fig. 8).

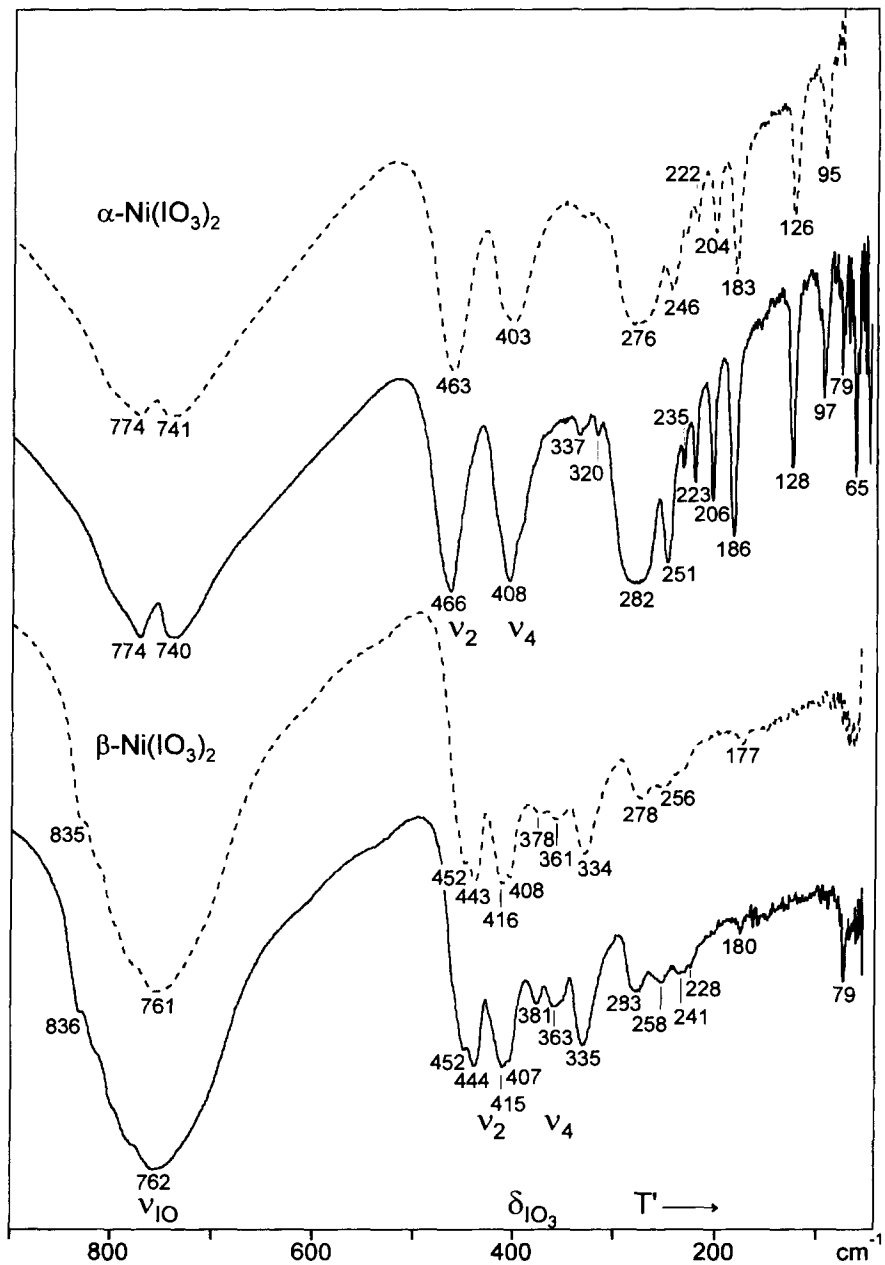

Fig. 7. Infrared spectra (KBr discs) of α- and β-$Ni(IO_3)_2$ at 90 and 300 K in the 50–900 cm^{-1} range (for further explanations see Figs. 2–4).

3.2. *Dehydration and phase transition of nickel iodates*

High-temperature Raman spectra, high-temperature X-ray diffraction patterns, and DSC curves of the title compounds are shown in Figs. 10–14. They reveal the progress of dehydration and decomposition of the hydrates under investigation as follows.

$Ni(IO_3)_2 \cdot 10H_2O$ is dehydrated to β-$Ni(IO_3)_2 \cdot 4H_2O$ above 298 K (see Figs. 10 and 12) (314 K, DSC

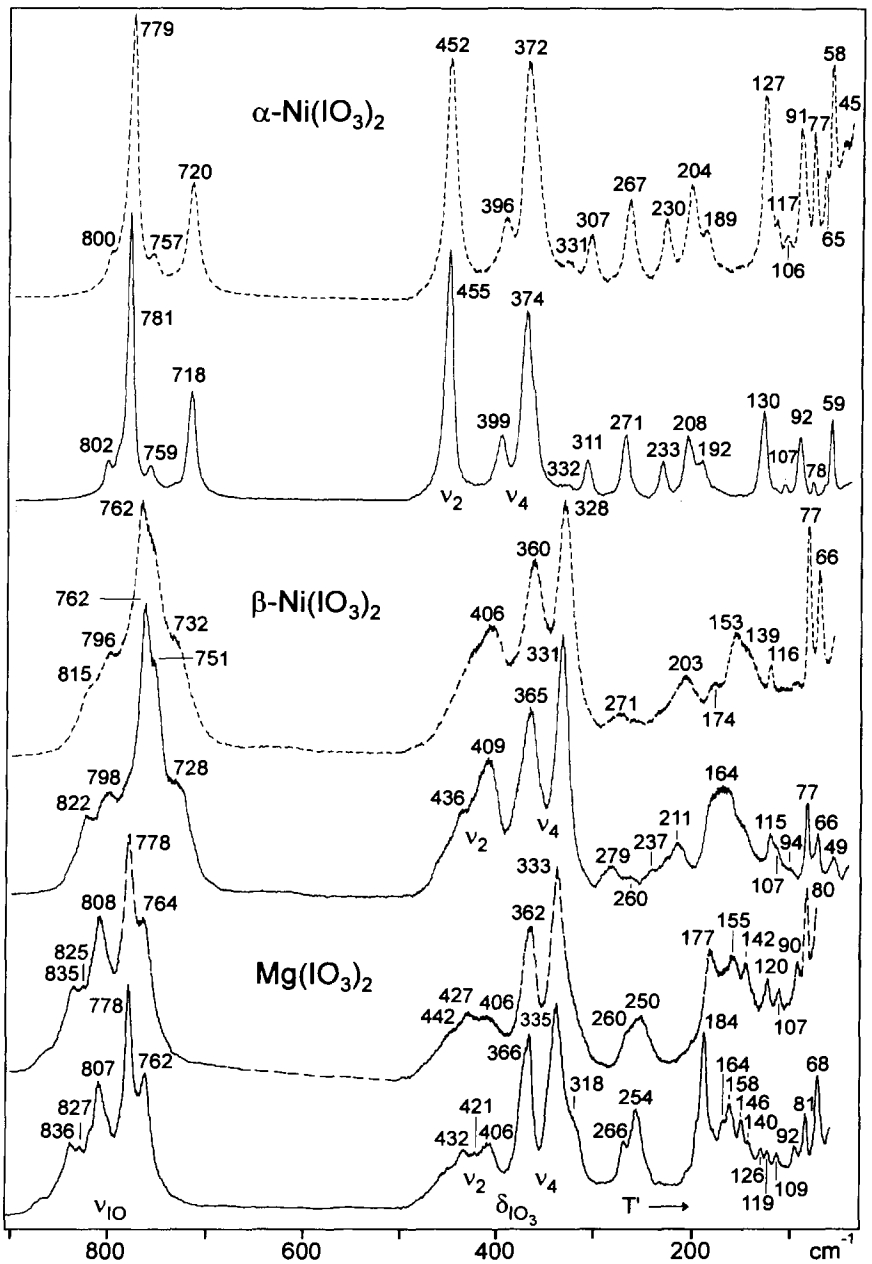

Fig. 8. Raman spectra of anhydrous $M(IO_3)_2$ (M = Ni, Mg) at 90 and 300 K in the 50–900 cm^{-1} range (for further explanations see Figs. 2–4).

intersection temperature). This is shown by an abrupt change of the Raman spectrum in the IO stretching mode region (two bands at 767 and 740 cm^{-1} instead of four at 799, 769, 755, and 741 cm^{-1}; see Fig. 10). α-$Ni(IO_3)_2{\cdot}4H_2O$ is dehydrated to the dihydrate at above 323 K (see Fig. 11) (384 K, DSC). This is revealed in the HT-Raman spectrum by two new bands at 379 and 127 cm^{-1}. Formation of α-$Ni(IO_3)_2{\cdot}4H_2O$ by decomposition of the decahydrate or transformation to the β-polymorph or reverse have never been

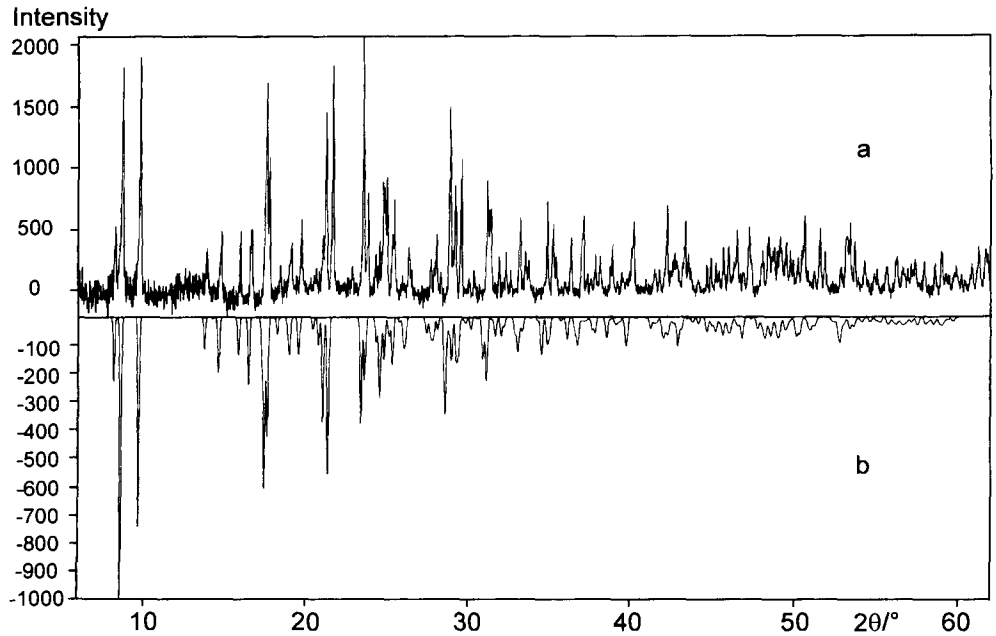

Fig. 9. X-ray diffraction pattern of $Ni(IO_3)_2 \cdot 10H_2O$ at 170 K; (a) – observed; and (b) – calculated via the fractional coordinates of the isostructural magnesium compound [22].

Table 1
Interplanar spacings d of α-$Ni(IO_3)_2 \cdot 4H_2O$ (in pm)

d_{exp}	I/I_0	d_{exp}	I/I_0	d_{exp}	I/I_0
1422.9	100	372.2	20	291.2	10
880.4	20	367.4	20	287.0	10
718.8	20	360.1	30	279.9	10
689.0	30	355.0	20	274.6	10
665.3	30	343.3	20	272.6	10
594.4	40	340.4	10	264.4	20
581.3	30	329.7	30	261.0	10
571.4	50	321.4	20	255.3	10
541.8	50	314.1	10	251.7	10
492.9	60	310.7	10	250.1	10
452.1	30	304.4	20	236.8	10
443.8	40	303.2	10	214.5	10
392.9	40	298.9	10		

Table 2
Interplanar spacings d of α-$Ni(IO_3)_2$ (in pm)

d_{exp}	I/I_0	d_{exp}	I/I_0	d_{exp}	I/I_0
504.91[a]	24	255.31	7	166.66	22
463.87	11	238.39[a]	8	159.44	7
443.09[a]	11	230.30[a]	12	147.63	8
371.67[a]	41	223.65	15	142.97	6
362.13[a]	53	211.31	26	141.50	7
344.13	100	204.49	7	125.42	9
328.94[a]	31	185.67	25	122.93	8
311.06[a]	10	181.61	10		
268.27[a]	41	169.03	8		

[a] Reflections corresponding to those reported in [16].

observed. β-$Ni(IO_3)_2 \cdot 4H_2O$ dehydrates to the dihydrate at 383 K (see Fig. 10) (421 K, DSC). This is especially shown by the increase in intensity of the band at 427 cm^{-1} and the decrease in intensity of the band at 97 cm^{-1} (Fig. 10). $Ni(IO_3)_2 \cdot 2H_2O$ is dehydrated to anhydrous α-$Ni(IO_3)_2$ at above 473K (see Figs. 10, 11 and 13) (431 K, DSC).

On heating above 700 K, α-$Ni(IO_3)_2$ transforms to the β-polymorph (see Fig. 13). Formation of green α-$Ni(IO_3)_2$ can be detected from the band at 721 cm^{-1} (see Fig. 10). Formation of the β-polymorph is connected with decomposition to NiO and iodine as shown by the I_2 overtone modes at 424, 636 and 844 cm^{-1} (Fig. 10). β-$Ni(IO_3)_2$ can neither be rehydrated, in contrast to α-$Ni(IO_3)_2$, nor transformed to the α-polymorph.

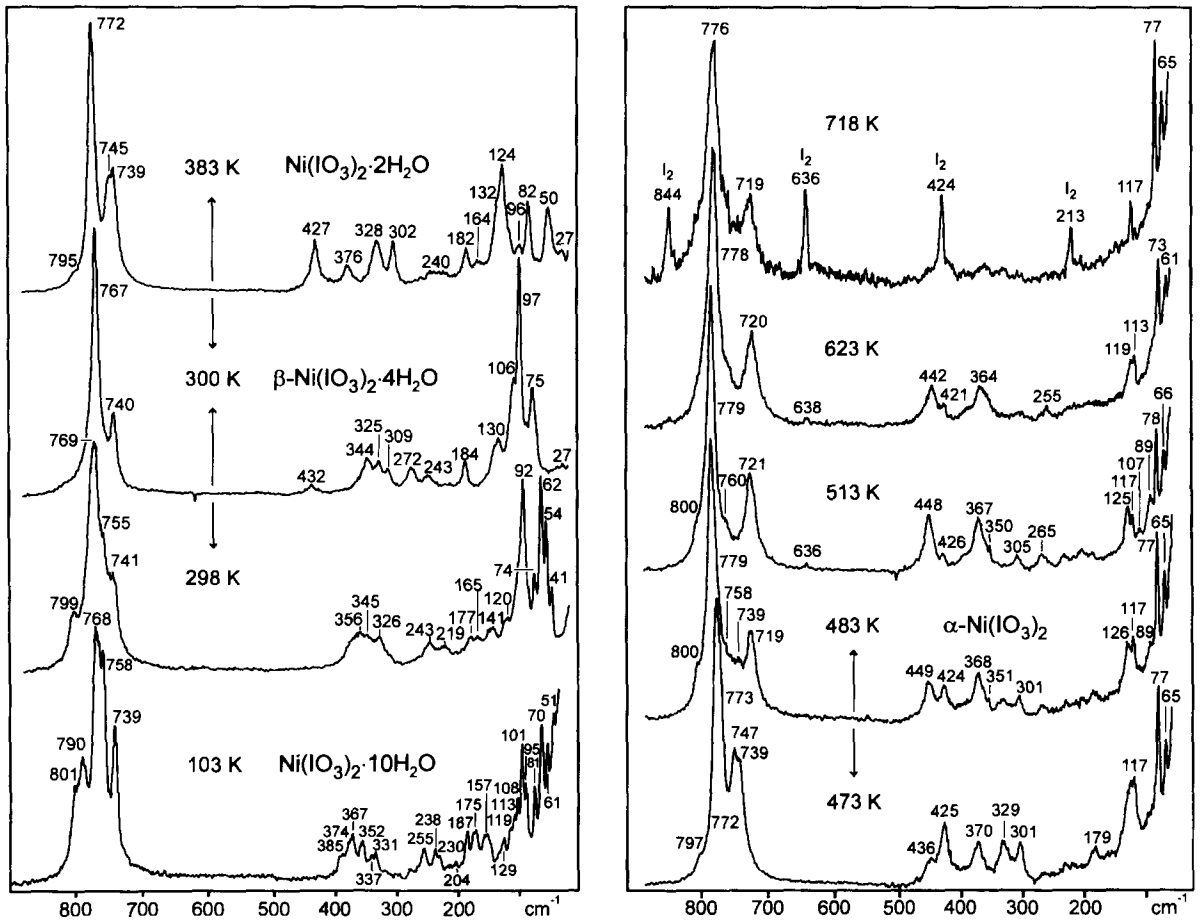

Fig. 10. High-temperature Raman spectroscopic dehydration studies of $Ni(IO_3)_2 \cdot 10H_2O$ in the 50–900 cm^{-1} range (open tube); arrows – dehydration or phase transition.

4. Discussion

4.1. Phase relationships

The results presented almost confirm dehydration, phase transition, and decomposition of the various nickel iodates as reported by Nassau et al. [7]. The phase relationships are presented in Fig. 15. The behaviour of $Ni(IO_3)_2 \cdot 10H_2O$ is included. We found two ways of dehydration in the system. The first one starts from $Ni(IO_3)_2 \cdot 10H_2O$ being comparable with the dehydration of $Mg(IO_3)_2 \cdot 10H_2O$. The other starts from α-$Ni(IO_3)_2 \cdot 4H_2O$. Mutual transformation of α-$Ni(IO_3)_2 \cdot 4H_2O$ and β-$Ni(IO_3)_2 \cdot 4H_2O$ was not observed. The temperatures of dehydration and phase transitions differ somewhat, depending on the experiments (DSC, HT-Raman, HT-X-ray) employed. This is mainly due to the different heating rates. The nature of some additional DSC peaks (in Fig. 14 marked with asterisks), which are not reflected by the HT-Raman and HT-X-ray experiments, is not yet known.

Which of the hydrates and anhydrous salts are thermodynamically stable, is not known so far. Nassau et al. [7] called the dihydrate the only stable compound in the presence of water, the tetrahydrates being intermediate metastable phases on the run to the stable compounds following the Ostwald step rule. On the other hand, $Ni(IO_3)_2 \cdot 10H_2O$ can only be prepared with some effort. In most cases, mixtures of both modifications are obtained. We therefore assume that

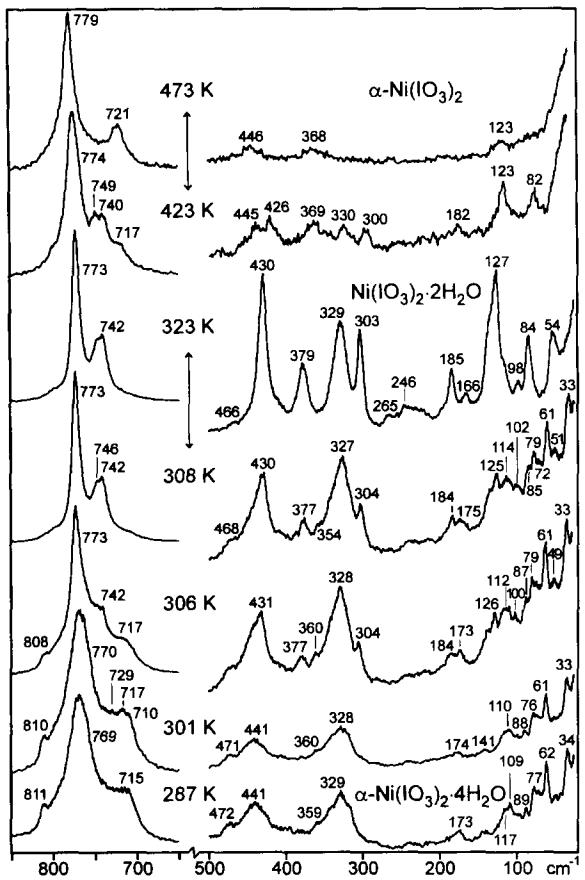

Fig. 11. High-temperature Raman spectroscopic dehydration studies of α-$Ni(IO_3)_2{\cdot}4H_2O$ in the 50–900 cm^{-1} range (for further explanations see Fig. 10).

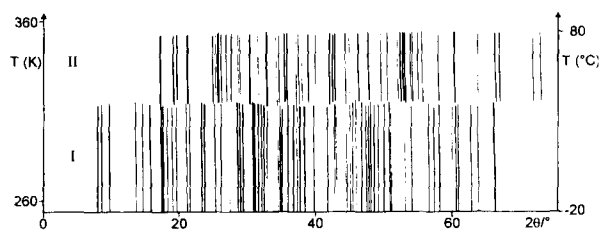

Fig. 12. High-temperature X-ray diffraction pattern (Cu$K\alpha_1$) of (I) – $Ni(IO_3)_2{\cdot}10H_2O$; and (II) – β-$Ni(IO_3)_2{\cdot}4H_2O$.

$Ni(IO_3)_2{\cdot}2H_2O$ is not the only stable phase. Of the two anhydrous compounds, however, the α-polymorph seems to be metastable at any temperature.

Decomposition of anhydrous nickel iodate to NiO, O_2, and I_2 resembles the behaviour of other transition

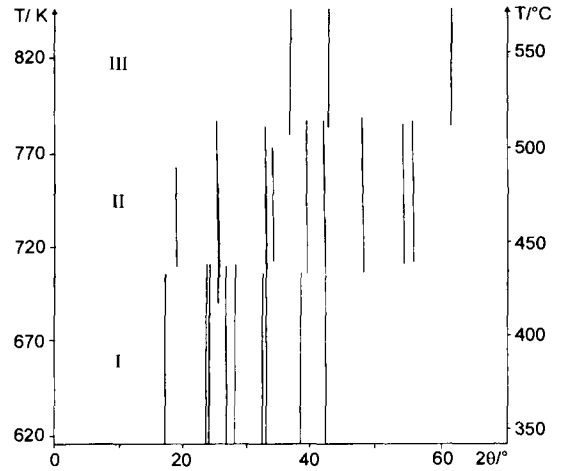

Fig. 13. High-temperature X-ray diffraction pattern (Cu$K\alpha_1$) of (I) – α-$Ni(IO_3)_2$; (II) – β-$Ni(IO_3)_2$; and (III) – NiO.

metal iodates. The reason for it lies in the larger stability of the respective oxides compared to that of the iodides, arising because of the small ionic radii of the respective metal ions, in contrast to the behaviour of the iodates of alkali and the heavier alkaline-earth metals [1–3].

4.2. IO_3 bending modes

Although IO stretching modes of the nickel iodates under study are in the range of other iodates (mean value of the Raman allowed IO stretches 769 cm^{-1} compared to 770 cm^{-1} of all iodates known [24]) the bending modes ν_2 and ν_4 are significantly shifted to higher wave numbers compared to 380 and 325 cm^{-1}, mentioned for alkali-metal iodates [25]. Thus, in the case of α-$Ni(IO_3)_2$, the symmetric bending mode ν_2 is observed at 452 (Raman) and 463 cm^{-1} (IR) (and at 400–440 cm^{-1} (Raman) for other nickel iodates (see Figs. 5–8)). The reason of this unusually great blue-shift is not easy to understand. Possibly, there is a decrease of the O–I–O angles and an increase of the bending force constants, which both give rise to a blueshift of the bending modes. The interpretation that the Raman bands under discussion have to be assigned to MO stretching modes [17], is doubtful. It is true, that metal–oxygen stretches can occur in that spectral region, if M are transition metals such as Ni or Cu, but surely not in the case of heavy entities such as iodate ions.

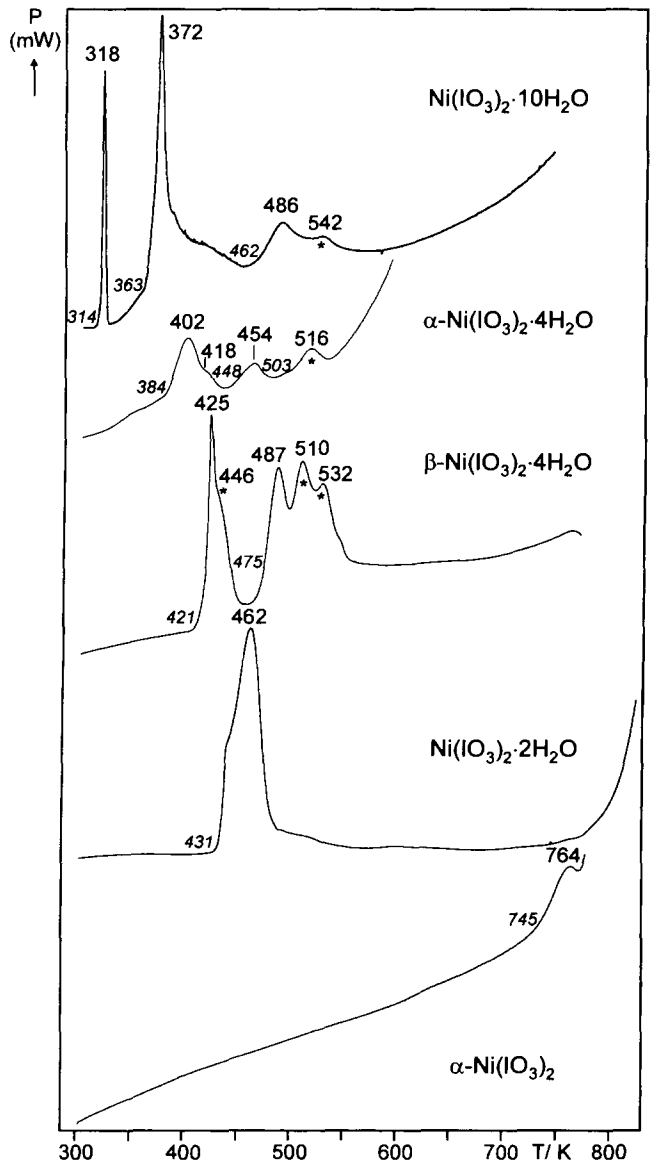

Fig. 14. DSC diagrams of nickel iodates (open crucible, heating rate – 10 K/min; figures, temperatures (K) of intersections (italic), and peak maxima (roman); peak at 372 K – evaporation of water and peaks at 450–490 K – decomposition of $Ni(IO_3)_2{\cdot}2H_2O$; asterisks – peaks not explained by high-temperature Raman and high-temperature X-ray experiments).

4.3. Hydrogen bonds

$Ni(IO_3)_2{\cdot}2D_2O$ is the only compound for which neutron diffraction studies have been performed [13]. The deuterium position established, however, only very crudely resembles those deduced from the spectroscopic data. Thus, the following intermolecular $H(D)\cdots O$ and intramolecular O–H(D) distances are calculated from the uncoupled O–D stretches (see Fig. 4) using the ν_{OD} vs. $r_{H(D)\cdots O}$ and $r_{O-H(D)}$ vs. ν_{OD} correlation curves reported in [26,27]: 190 and 179 pm, and 96.2 and 97.3 pm instead of 202 and 168 pm, and 95 and 97 pm [13], respectively.

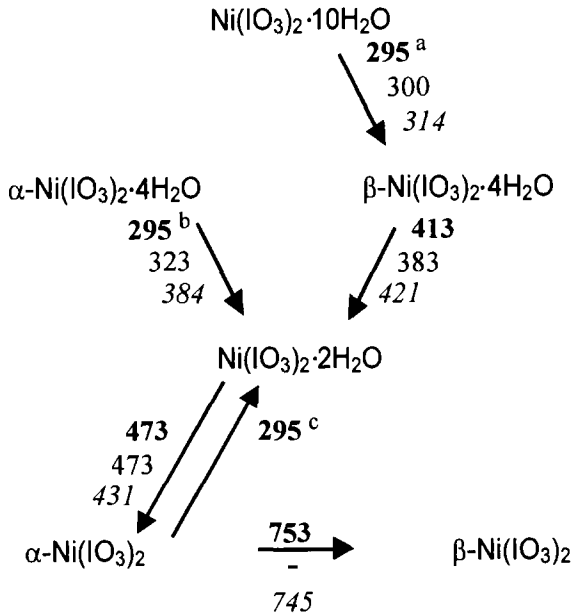

Fig. 15. Phase relationships of nickel iodates; figures – transition temperatures (K); bold types – preparation procedures (see text); Roman - High-temperature Raman spectra; italic – DSC data; a – within 10 min on air; b – within some days on air; and c – in an aqueous solution.

References

[1] Z. Gontarz and A. Górski, Roczn. Chem., 48 (1974) 2091.
[2] M. Maneva, M. Georgiev, N. Lange and H.D. Lutz, Z. Naturforsch., 46b (1991) 795.
[3] E. Alici, Th. Schmidt and H.D. Lutz, Z. Anorg. Allg. Chem., 608 (1992) 135.
[4] D. Weigel, B. Imelik and M. Prettre, Bull. Soc. Chim. Fr., 1962 (1962) 1427.
[5] Gmelin Handbook, 57 Ni B2, (1966) p. 624.
[6] A. Meusser, Berichte d. D. Chem. Gesellschaft, 34 (1901) 2432.
[7] K. Nassau, J.W. Shiever and B.E. Prescott, J. Solid State Chem., 7 (1973) 186.
[8] E.H.P. Cordfunke, J. Inorg. Nucl. Chem., 35 (1973) 2699.
[9] J.B.A.A. Elemans and G.C. Verschorr, J. Inorg. Nucl. Chem., 35 (1973) 3183.
[10] S.C. Abrahams, R.C. Sherwood, J.L. Bernstein and K. Nassau, J. Solid State Chem., 7 (1973) 205.
[11] M. Maneva and V. Koleva, J. Thermal Anal., 41 (1994) 817.
[12] K. Nassau, J. Crystal Growth, 15 (1972) 171.
[13] J.B.A.A. Elemans, B. van Laar and B.O. Loopstra, Physica, 57 (1972) 215.
[14] S.C. Abrahams, J.L. Bernstein, J.B.A.A. Elemans and G.C. Verschorr, J. Chem. Phys., 59 (1973) 2007.
[15] L. Jianmin, Z. Yongfeng and F. Jifa, Cryst. Res. Technol., 21 (1986) 1595.
[16] C. Svensson, S.C. Abrahams and J.L. Bernstein, J. Solid State Chem., 36 (1981) 195.
[17] W.E. Dasent and T.C. Waddington, J. Chem. Soc. (1960) 2429.
[18] H.D. Lutz, H. Möller and M. Schmidt, J. Mol. Struc., 328 (1994) 121.
[19] K. Beckenkamp, Doctoral Thesis, Univ. Siegen, 1991.
[20] LSUCR, Least Squares Unit Cell Refinement, Programm Bibliothek RRZ Köln.
[21] K. Yvon, W. Jeitschko and E. Parthé, J. Appl. Cryst., 10 (1977) 73.
[22] E. Suchanek, Z. Zhang and H.D. Lutz, Z. anorg. allg. Chem., 622 (1896) 1957.
[23] H. Möller, E. Suchanek, H.D. Lutz and W. Paulus, Z. Naturforsch., 49b (1994) 1334.
[24] Th. Kellersohn, E. Alici, D. Eßer and H.D. Lutz, Z. Kristallogr., 203 (1993) 225.
[25] W.E. Klee, Spectrochim. Acta, 26A (1970) 1165.
[26] W. Mikenda, J. Mol. Struct., 147 (1986) 1.
[27] H.D. Lutz, C. Jung, J. Mol. Struct., in press.